Full Paper
Journal of Nano Materials Impact 2026, 02 (01) 22-28

Nanoparticle-Mediated Dose Enhancement in Radiotherapy: A Reproducible Workflow to Jointly Quantify DEF and SER

Haneen Abass Alrubaie*[,1], Raneen Salam[1], Alyaa Hussein Ashour[2]
[1]Al-Nahrain Renewable Energy Research Center, Al-Nahrain University, Baghdad, IRAQ. [2]College of Medicine, Al-Nahrain University, Baghdad, IRAQ.

Abstract

There has been growing interest in the use of nanoparticles to radiosensitise tumours, as this technique has the potential to maximise the radiation dose delivered within a tumour while minimising the dose delivered to surrounding healthy tissue. In this context, this study provides a reproducible methodology to evaluate the dose enhancement factor (DEF) and the sensitizer enhancement ratio (SER) simultaneously under clinical photon-beam conditions. The methodology combines reference dose measurements with an ionisation chamber, dose mapping with Gafchromic EBT3 films, region-of-interest (ROI) analysis, radiotherapy dose-data processing using the DICOM RTDose standard, uncertainty estimation, and linear-quadratic modelling of cell survival. This integration provides a structured and standardised framework for comparable reporting of physical and biological enhancement indices across different studies. Instead of presenting the experimental dataset as a novel biological validation, it was analysed to demonstrate the applicability of the proposed methodology. The obtained results showed that gold nanoparticles produced DEF values of 1.35 at 120 kVp and 1.05 at 6 MV, whereas titanium dioxide (TiO_2) nanoparticles produced corresponding values of 1.15 and 1.03, respectively. The calculated SER values were 1.20 and 1.10 for gold and TiO_2 nanoparticles, respectively, at a cell-survival level of 0.1 under the studied conditions. Overall, the proposed workflow provides a clear and transparent platform for standardising reports of nanoparticle-mediated radiotherapy enhancement, enabling replication and comparison in future studies.

Keyword: Gold nanoparticles • TiO_2 • dose enhancement factor • sensitizer enhancement ratio • reproducible protocol.

Introduction

The response to radiotherapy is critically influenced by the tolerance of healthy tissue to the dose and by the properties of the tumour microenvironment, including hypoxia and the heterogeneity of the radiation response of tumour cells. As a result, radiosensitisation with the use of nanoparticles is an important area of research, with the aim of increasing radiation damage within the tumour without increasing the total dose to healthy tissues. One of the most commonly used radiosensitizers is gold nanoparticles. Gold has a high atomic number, and therefore the probability of photoelectric reactions, especially at kilovolt energies, is increased. In contrast, titanium dioxide nanoparticles have been paid special attention due to their ability to promote the generation of reactive oxygen species induced by radiation, contributing to the activation of oxidative damage pathways in tumour cells[1-8]. Despite the abundance of published studies on this topic, the differences in the methodology of these studies still make it difficult to compare them accurately and apply these techniques in practice. Many studies use the terms ‘dose enhancement’ and ‘radiosensitisation’ synonymously, but there are variations between studies in the methods of film calibration, region of interest (ROI) definition, beam quality characterisation and reporting of uncertainties[9-12]. Therefore, differences reported between studies may be attributed to differences in analytical methods, such as calculating the average dose within the ROI, recording dose maps, or matching survival curves, rather than actual differences related to the type of nanomaterial or its mechanism of action. The current protocol fills this gap by providing a systematic approach to reporting both the dose enhancement factor (DEF) and the sensitisation enhancement ratio (SER) under a single measurement framework and unambiguous analytical assumptions.

The aim of this study is to propose a standardised and reproducible workflow to estimate and report the DEF and the SER under the same geometrical and analytical conditions. The numerical tables in this paper do not result from an independent experimental verification campaign. Instead, this data is used as an example dataset to demonstrate the calibration steps, extraction of region-of-interest data, analysis of the dose-volume curves, and processing of radiotherapy dose data according to the DICOM RTDose standard. In addition, uncertainty propagation was calculated, and a linear-quadratic model was used[13-15]. This framework offers a practical and structured basis for the production of auditable and comparable reports in studies on radiotherapy enhancement with nanoparticles.

***Address for correspondence** Asst. Lect. Haneen Abass Alrubaie, Renewable Energy Research Center, Al-Nahrain University, Baghdad, Iraq.

E-mail: haneen_a@nahrainuniv.edu.iq

ORCID: https://orcid.org/0009-0007-9294-9000

Info:
Submitted: 01 Jan. 2026; **Revised:** 25 Jan. 2026;
Accepted: 11 Feb. 2026; **Published:** 15 Feb. 2026.
https://doi.org/10.71109/nmi.2026.2.1.19

Background And Theory

Physical Mechanisms and Energy Dependence

At diagnostic and orthovoltage energies, the photoelectric absorption probability increases approximately with atomic number according to the relationship Z^n/E^3, where n typically ranges between 3 and 4 depending on the energy range. Therefore, high-atomic-number materials, such as gold, are more capable of enhancing photon absorption and producing a large number of low-energy secondary electrons. These electrons have short ranges within the biological medium, including electrons produced by Auger cascades, allowing the formation of localized high-dose regions at the nanoscale near nanoparticle surfaces. However, the measured macroscopic effect depends not only on material type but also on nanoparticle concentration, spatial distribution within the sample or tumour, and the radiation-beam spectrum. Therefore, the apparent enhancement may be reduced when the dose is averaged over relatively large regions of interest, such as millimetre-scale ROIs. At megavoltage energies, Compton scattering becomes the dominant interaction mechanism, reducing the dependence on the atomic number of the material. Consequently, macroscopic dose enhancement factor (DEF) values may be close to unity, even in cases where clear biological enhancement of the radiation response is observed[1, 4, 9-12].

Chemical and Biological Mechanisms

In addition to purely physical interactions, nanoparticles can modify the chemical stage of radiation action by enhancing reactive oxygen species (ROS) production, influencing water-radiolysis pathways, and affecting oxygen-related chemistry. AuNPs may increase oxidative stress and alter DNA repair signalling, while TiO_2 can catalyse ROS generation under suitable irradiation conditions. These pathways help explain why biological enhancement may persist even when macroscopic DEF is modest[5-9].

Definitions: DEF, LQ survival, and SER

The macroscopic dose enhancement factor is defined for a fixed geometry and ROI as:

$$DEF = \frac{D_{NP}}{D_{CTRL}} \quad \text{... (1)}$$

where D_{NP} and D_{CTRL} are the mean absorbed doses (Gy) in the ROI for the nanoparticle-treated and control conditions, respectively.

Clonogenic survival is modeled using the linear-quadratic (LQ) relationship:

$$SF(D) = \exp[-(\alpha D + \beta D^2)] \quad \text{... (2)}$$

where SF is the surviving fraction at dose D, and α and β are fitted radiosensitivity parameters.

The sensitizer enhancement ratio at a chosen surviving fraction SF* is defined as.

$$SER(SF^*) = \frac{D_{CTRL(SF^*)}}{D_{NP(SF^*)}} \quad \text{... (3)}$$

where $D_{CTRL(SF^*)}$ and $D_{NP(SF^*)}$ are the doses required to reach SF* in the control and nanoparticle-treated conditions, respectively, as derived from the fitted LQ curves.

Because DEF depends on the selected ROI and spatial averaging, and SER depends on the chosen surviving-fraction level and the stability of the linear-quadratic fit, both quantities should be interpreted as comparative workflow metrics rather than universal material constants.

Reporting and Uncertainty

To support meaningful comparison, the workflow reports beam quality (kVp spectrum or MV nominal energy plus field size), ROI definition and spatial resolution, dosimeter calibration and readout conditions, and an explicit uncertainty budget covering calibration, setup, registration, and biological variability. In addition, DEF is interpreted as an ROI-dependent dosimetric endpoint and SER as an LQ-model-dependent biological endpoint rather than as universal material constants. If D_{NP} and D_{CTRL} are treated as independent, the uncertainty in DEF can be approximated by standard propagation.

$$\frac{u_{DEF}}{DEF} = \sqrt{\left[\left(\frac{u_{DNP}}{D_{NP}}\right)^2 + \left(\frac{u_{DCTRL}}{D_{CTRL}}\right)^2\right]} \quad \text{... (4)}$$

Survival-curve uncertainty was considered to arise from plating efficiency, colony counting, and inter-experiment variability[13-15]

Materials and Methods

Nanoparticles and Preparation

For the workflow demonstration, AuNP conditions were defined as citrate- or PEG-stabilized colloids with nominal diameters of 10, 30, and 50 nm. TiO_2 conditions were defined as anatase or mixed-phase nanoparticles within a comparable size range. Dispersions were prepared in sterile aqueous media at 0, 50, 100, and 200 μg/mL and were sonicated immediately before irradiation to minimize aggregation.

Irradiation Beams and Geometry

Two photon qualities were selected to separate physical from chemical and biological contributions: (i) 120 kVp X-rays, for which photoelectric enhancement is pronounced, and (ii) 6 MV photons, for which Compton interactions dominate. The field size, source-to-surface distance, buildup conditions, and phantom material were defined for each configuration. For cell-related measurements, a water-equivalent phantom and a standardized culture-plate holder were used to improve reproducibility and alignment with clinical reference conditions. In the present workflow, geometry was reported explicitly. The reference configuration used a 10 cm × 10 cm field at SSD = 100 cm for 6 MV with water-equivalent buildup to a 5 cm measurement depth, together with an orthovoltage setup in which filtration/HVL and detector depth were documented under matched phantom conditions.

Dosimetry: Ion Chamber and Film Mapping

The reference dose was determined using an ionization chamber, taking into account the beam quality and approved experimental geometry, and in accordance with established institutional dosimetry protocols. For two-dimensional dose mapping, Gafchromic EBT3 film was used under standardized processing procedures that included preheating the scanner, fixing the film orientation during scanning, and acquiring 48-bit RGB images, while adhering to a fixed post-irradiation waiting period as per the manufacturer's instructions. A multi-point calibration curve was generated for each batch of films, and the film's response was then converted to an absorbed dose based on an appropriate calibration model. The film dose maps were then recorded and matched to the defined region of interest (ROI), and the average dose within the ROI was calculated to extract the D_{NP} and D_{CTRL} values, which were subsequently used to calculate the dose enhancement factor (DEF)[16-18]. To minimize ambiguity in DEF reporting, the ROI was geometrically defined, and its dimensions and position were fixed so that it would be applied in the same way under all measurement conditions. In the phantom- and film-based measurements, a central square ROI measuring 10 mm × 10 mm was used within a region of suitable dose homogeneity. In the plate irradiation experiments, the irradiated well was chosen as the ROI to ensure that the extracted dose was as representative as possible of the actual area being analysed.

The scanning and reporting settings were kept the same during the analysis for better reproducibility of the results. All automatic colour corrections were disabled and a transmission-mode flatbed scanner, an Epson Expression 10000XL/12000XL or equivalent, with 48-bit RGB acquisition at 150 dpi was used. Film orientation was determined with a fixed marker, and the scanner was allowed 30 minutes of warm-up time before scanning. All films were scanned simultaneously after irradiation following the manufacturer's instructions and the calibration chart applied in this study (See **Figure 1**).

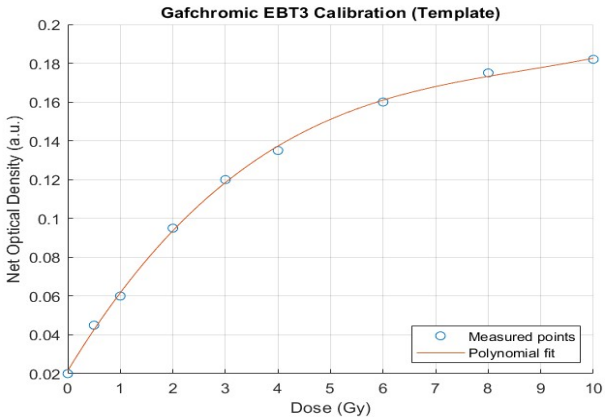

Figure 1. Gafchromic EBT3 calibration curve used to convert scanner response (net optical density) to absorbed dose. In the present workflow, calibration was performed for each film lot under identical scanner settings and post-irradiation timing to preserve traceable dose conversion.

Biological Endpoints and Clonogenic Assay

Prior to irradiation, cells were treated with nanoparticles at defined concentrations and exposure times. After irradiation, cells were seeded at precalculated densities and incubated for a sufficient time to form colonies. The biological evaluation was then performed by determining the number of colonies formed, with correction for plating efficiency, to calculate the surviving fraction.

The reproducible component of the protocol documented the cell line used, the duration of cell incubation with nanoparticles, the irradiation dose points (0–8 Gy), the seeding density used for each dose, and the criteria for colony staining and counting. The number of independent biological replicates used in the analysis was also recorded to improve the reliability and comparability of the results.

MATLAB Analysis Pipeline (DICOM RT Dose, DVH, DEF, LQ)

The analysis included the following steps: (1) loading the RT Dose DICOM file and calculating the absolute dose in gray (Gy) using Dose Grid Scaling; (2) defining region-of-interest (ROI) masks for the phantom region or cell-plate region and calculating the mean or median dose and dose-volume histograms (DVHs); (3) deriving DEF values from the mean doses in the ROIs; (4) fitting the linear-quadratic coefficients to the clonogenic cell-survival data; and (5) calculating SER at the selected surviving fraction. All scripts for unit conversion, ROI extraction, and model fitting were version-controlled and implemented using fixed input conventions for reproducibility (See **Figure 2**).

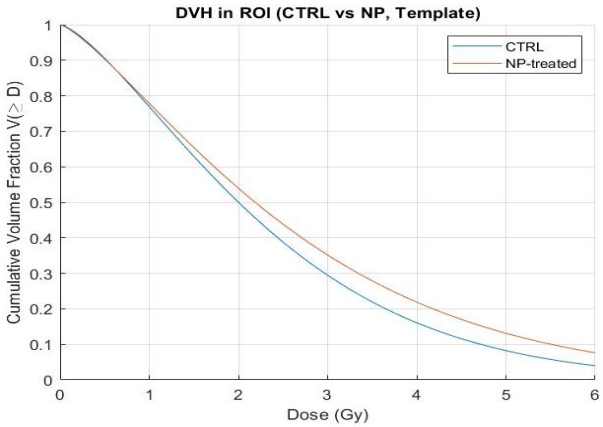

Figure 2. Dose-volume histogram (DVH) within the selected ROI showing the reporting format used to compare control and nanoparticle-treated conditions. This DVH-based presentation provides a compact comparison of central tendency and heterogeneity within the standardized ROI.

Study Design and Dataset

Tables 1–4 report the study design, uncertainty components and quantitative outputs used to report the total dose enhancement factor (DEF) and bioradiosensitisation indices, including the linear-quadratic model (LQ) coefficients and the sensitiser enhancement ratio (SER). The general design of the study included the type, size, and concentration of nanoparticles, and the quality of the radiation beam represented by the photon beams of 120 kVp and 6 MV. The

numbers presented in **Tables 3** and **Table 4** are examples of data used to illustrate the reporting structure and the analytical steps and should not be taken as a substitute for an independent and comprehensive experimental verification study.

Table 1. Study design factors and levels.

Factor	Levels
NP type	None (CTRL); Au; TiO_2
Size (nm)	10; 30; 50
Concentration (µg/mL)	0; 50; 100; 200
Beam quality	120 kVp; 6 MV
Endpoints	DEF; DVH metrics; SF_2; LQ (α, β); SER at SF = 0.1

Table 2. Example uncertainty budg.

Component	Typic alrelative uncertainty
Film calibration (lot-specific)	3%
Scanner repeatability / positioning	2%
ROI registration / alignment	4%
Setup reproducibility	3%
Colony counting and plating efficiency	5%

Table 3. Macroscopic DEF values. (conservative σ propagated using Eq.(4) with typical components in Table 2).

Condition	Beam	Meandose CTRL (Gy)	Meandose NP (Gy)	DEF	DEF(±σ,k=1)
Au 30 nm, 200 µg/mL	120 kVp	2.00	2.70	1.35	1.35± 0.12
Au 30 nm, 200 µg/mL	6 MV	2.00	2.10	1.05	1.05± 0.09
TiO_2 30 nm, 200 µg/mL	120 kVp	2.00	2.30	1.15	1.15± 0.10
TiO_2 30 nm, 200 µg/mL	6 MV	2.00	2.06	1.03	1.03± 0.09

Table 4. LQ fit parameters and SER (SF* = 0.1).

Condition	α (Gy^{-1})	β (Gy^{-2})	SF2	SER@SF=0.1
CTRL	0.30	0.030	0.55	1.00
Au 30 nm, 100 µg/mL	0.38	0.035	0.48	1.20
TiO_2 30 nm, 200 µg/mL	0.34	0.032	0.52	1.10

Results And Discussion

Physical Dose Enhancement Trends (DEF)

The dose enhancement factor (DEF) is defined as the ratio of the mean absorbed dose inside the same region of interest (ROI) with nanoparticles present to the mean absorbed dose under control conditions, as given in Equation (1). In the illustrative dataset, DEF increased substantially at 120 kVp, while the change was modest at 6 MV. The observed behaviour is in agreement with the expected crossover from a stronger photoelectric contribution at lower energies to interactions dominated by Compton scattering in MV beams[1, 4, 10-12]. In particular, this trend confirms that the calibration steps, ROI identification, and DEF extraction in the proposed methodology preserve the well-established beam-energy dependence of nanoparticle-mediated physical enhancement. The change in the dose enhancement factor (DEF) with nanoparticle concentration is summarised in **Figure 3.**

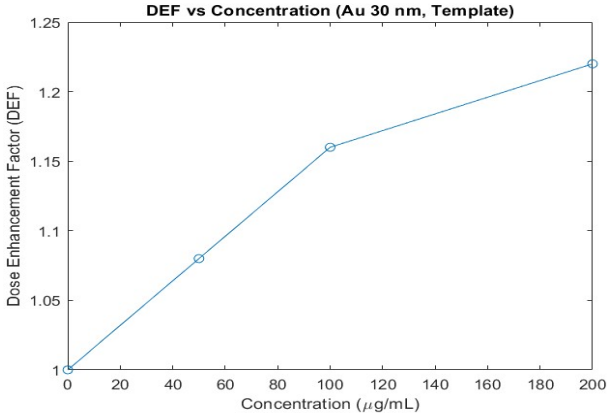

Figure 3. Dose enhancement factor (DEF) as a function of nanoparticle concentration for Au and TiO_2 under 120 kVp and 6 MV beams. The trend highlights stronger enhancement at 120 kVp and near-unity DEF at 6 MV, consistent with photoelectric versus Compton dominance.

Size Dependence at Fixed Loading

At a constant concentration, the size of nanoparticles can influence energy deposition, absorption, and spatial distribution mechanisms, as well as their potential for aggregation within the medium. This can be reflected in the calculated dose measurements within the region of interest, even when the amount of nanomaterial added is constant. Although the dose enhancement factor (DEF) represents a spatially averaged value within the region of interest, variations in particle size, distribution, and beam spectrum can lead to significant changes in the measured enhancement. **Figure 4** illustrates the variation in DEF values as a function of nanoparticle diameter at a constant concentration.

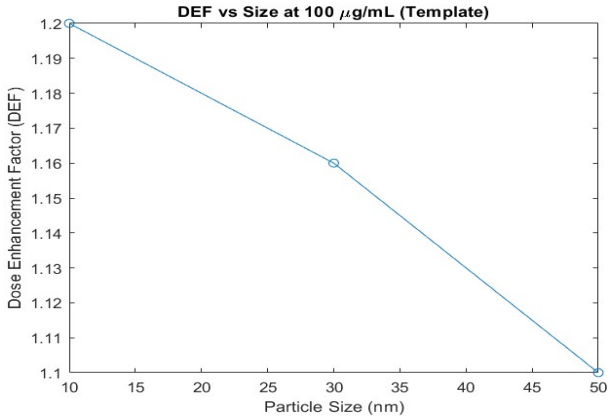

Figure 4. DEF as a function of particle diameter at fixed concentration (reported using the standardized ROI definition). Although DEF is ROI-averaged, size-dependent differences may reflect clustering, microdistribution, and spectrum-dependent effects at fixed loading.

Biological Radiosensitization (LQ survival and SER)

The radiosensitivity of the cells was assessed using cell-survival curves fitted to the linear-quadratic (LQ) model, as shown in Equation (2). Compared with the control group,

treatments based on gold nanoparticles and titanium dioxide showed clear changes in the fitted radiosensitivity coefficients, accompanied by a decrease in SF_2 values, as shown in **Table 4.** Within the proposed workflow, **Figure 5** illustrates the conversion of cell-survival data into standardised LQ fits and then into SER values, allowing direct comparison between different experimental conditions.

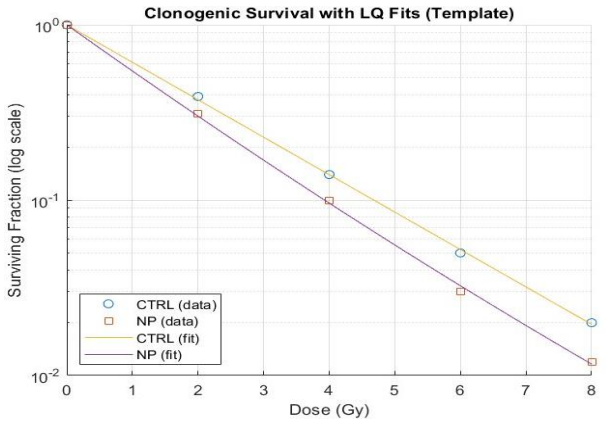

Figure 5. Clonogenic surviving fraction versus dose for control and nanoparticle-treated conditions with linear-quadratic (LQ) fits. The fitted curves are used to extract SF_2 and to solve for the dose at the selected SF* employed in SER computation.

SER at A Fixed Surviving Fraction (SF* = 0.1)

SER provides a single-number summary of biological enhancement at a fixed surviving fraction, SF* (Eq. 3). In the demonstration dataset, SER at SF = 0.1 reached 1.20 for Au (30 nm, 100 µg/mL) and 1.10 for TiO_2 (30 nm, 200 µg/mL) **Table 4. Figure 6** summarizes the SER values for the investigated conditions. The methodological contribution of this protocol is based on the joint reporting of DEF and SER. DEF may be close to unity under high-energy (MV) beams within the combined uncertainty range of dose measurement and registration, while SER may remain above 1 because chemical and biological mechanisms operate at sub-ROI scales. Reporting both measures together, with a clear ROI definition and uncertainty budget, clarifies whether the observed behaviour mainly reflects macroscopic dose measurement or the subsequent biological response, thereby enabling benchmarking between studies under identical analytical assumptions.

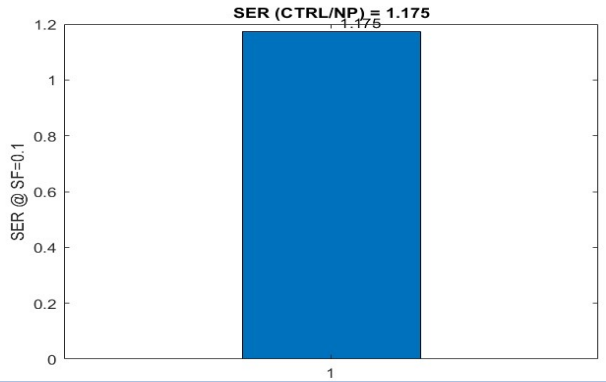

Figure 6. Sensitizer enhancement ratio (SER) evaluated at SF* = 0.1 across the investigated nanoparticle conditions. SER summarizes biological enhancement at SF* = 0.1, enabling direct comparison even when macroscopic DEF is close to unity.

Uncertainty Budget and Reproducibility

Sources of uncertainty in DEF and SER values include dosimetric factors (film calibration, scanner repeatability, setup reproducibility, and ROI registration) and biological factors (plating efficiency and colony counting). Registration and biological variability may dominate and mask minor MV improvements, as summarised in **Table 2**; therefore, reliable interpretation requires adequate sample size, rigorous controls, and consistent handling. Explicit uncertainty calculation also enhances reproducibility, as it allows different laboratories to determine whether the reported differences exceed the main sources of measurement uncertainty. The relative uncertainties are summarised in **Figure 7**.

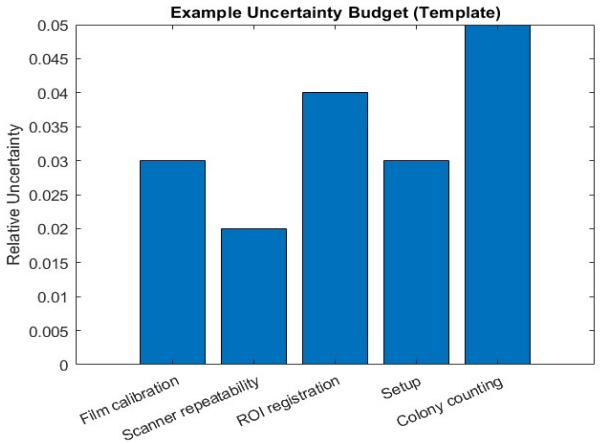

Figure 7. Relative-uncertainty budget highlighting dominant contributors in dosimetry and clonogenic analysis. The plot emphasizes that ROI registration and biological variability can dominate total uncertainty, particularly for MV beams.

In summary, the demonstration data show the expected qualitative behaviour: the dose enhancement factor (DEF) is higher at 120 kVp than at 6 MV, especially for high-atomic-number gold (Au), due to enhanced photoelectric interactions[1, 4, 10-12]. Although the macroscopic DEF approaches unity at 6 MV, a small but non-zero SER effect may still occur, consistent with the contributions of nanoscale energy deposition, intracellular localization, and ROS-mediated chemical reactions to megavoltage radiosensitisation[3-9]. The results therefore provide an important validation of the reporting workflow and its explanatory logic, illustrating why DEF and SER should be reported together with ROI size, spatial resolution, and uncertainty information.

Limitations and Practical Notes

Several limitations must be considered when applying and interpreting nanoparticle radiosensitisation measurements. Aggregation and deposition can lead to irregular nanoparticle distributions, affecting both physical dose mapping and biological response. Scanner settings and post-irradiation film-response evolution affect film dosimetry measurements; therefore, batch-specific calibration and consistent handling are essential[16-18]. DEF values derived from DICOM RTDose data and ROI masks depend on registration accuracy, and even minor deviations in ROI placement can increase uncertainty. SER depends on the validity of the LQ model

within the studied dose range. Therefore, both DEF and SER should be interpreted within the defined ROI and model assumptions and should not be considered general physical constants. Finally, clinical application requires consideration of toxicity, pharmacokinetics, and tumour targeting, which are outside the scope of this protocol but critical for subsequent studies[19-21].

For orthovoltage beams, film response and calibration may be more sensitive to beam quality, including filtration and half-value layer (HVL), than in megavoltage beams. Therefore, the calibration was matched to the beam quality used in the measurements and is reported with filtration/HVL data where available.

Future work will involve validating the entire workflow using independent mock measurements and laboratory datasets for multiple beam qualities, as well as sharing programmed analytical resources to facilitate external replication and benchmarking.

Conclusion

Here, we report a reproducible and verifiable method to measure nanoparticle-mediated dose enhancement and radiosensitisation for clinically relevant photon beams. This methodology is based on reference dosimetry using an ionisation chamber, EBT3 film mapping, standardised region-of-interest (ROI) analysis, dose-volume histogram analysis, and LQ-based clonogenic survival modelling. It yields two complementary endpoints: the macroscopic dose enhancement factor (DEF) and the biological sensitizer enhancement ratio (SER).

The main value of this work is methodological and educational. The manuscript proposes a standardised approach for defining, measuring, analysing, and reporting dose enhancement and radiosensitisation with explicit assumptions about the ROI and uncertainty. The numerical examples presented are intended to illustrate this methodology and should not be taken as an independent experimental validation. Consequently, the study provides a practical reporting framework that can support more reproducible comparisons in future nanoparticle radiotherapy studies.

Acknowledgements

None.

Funding

The authors declare that no external funding was received for this study.

Authorship Contribution

Haneen Abass Alrubaie contributed to the study design, methodology development, data analysis, manuscript writing, and final revision of the manuscript.

Raneen Salam contributed to data interpretation, manuscript review, and scientific discussion.

Alyaa Hussein Ashour contributed to methodology support, technical review, and manuscript revision.

Declaration of Competing Interests

The authors declare that they have no conflicts of interest.

References

[1] K. T. Butterworth, S. J. McMahon, F. J. Currell, and K. M. Prise, "Physical basis and biological mechanisms of gold nanoparticle radiosensitization," *Nanoscale*, vol. 4, no. 16, p. 4830–4838, 2012. https://doi.org/10.1039/c2nr31227a.

[2] J. F. Hainfeld, F. A. Dilmanian, D. N. Slatkin, and H. M. Smilowitz, "Radiotherapy enhancement with gold nanoparticles," *Journal of Pharmacy and Pharmacology*, vol. 60, no. 8, p. 977–985, 2008. https://doi.org/10.1211/jpp.60.8.0005.

[3] S. Jain *et al.*, "Cell-Specific Radiosensitization by Gold Nanoparticles at Megavoltage Radiation Energies," *International Journal of Radiation Oncology, Biology, Physics*, vol. 79, no. 2, p. 531–539, 2011. https://doi.org/10.1016/j.ijrobp.2010.08.044.

[4] S. H. Cho, B. L. Jones, and S. Krishnan, "The dosimetric feasibility of gold nanoparticle-aided radiation therapy (GNRT) via brachytherapy using low-energy gamma-/x-ray sources," *Physics in Medicine & Biology*, vol. 54, no. 16, p. 4889, 2009. https://doi.org/10.1088/0031-9155/54/16/004.

[5] B. L. Jones, S. Krishnan, and S. H. Cho, "Estimation of microscopic dose enhancement factor around gold nanoparticles by Monte Carlo calculations," *Medical Physics*, vol. 37, no. 7Part1, p. 3809–3816, 2010. https://doi.org/10.1118/1.3455703.

[6] D. Howard, S. Sebastian, Q. V. Le, B. Thierry, and I. Kempson, "Chemical Mechanisms of Nanoparticle Radiosensitization and Radioprotection: A Review of Structure-Function Relationships Influencing Reactive Oxygen Species," *International Journal of Molecular Sciences*, vol. 21, no. 2, p. 579 https://doi.org/10.3390/ijms21020579

[7] M. Nakayama, H. Akasaka, R. Sasaki, and M. Geso, "Titanium Dioxide-Based Nanoparticles to Enhance Radiation Therapy for Cancer: A Literature Review," *Journal of Nanotheranostics*, vol. 5, no. 2, pp. 60–74 https://doi.org/10.3390/jnt5020004

[8] K. Morita *et al.*, "Titanium oxide nano-radiosensitizers for hydrogen peroxide delivery into cancer cells," *Colloids and Surfaces B: Biointerfaces*, vol. 198, p. 111451, 2021. https://doi.org/10.1016/j.colsurfb.2020.111451.

[9] S. J. McMahon *et al.*, "Biological consequences of nanoscale energy deposition near irradiated heavy atom nanoparticles," *Scientific Reports*, vol. 1, no. 1, p. 18, 2011. https://doi.org/10.1038/srep00018.

[10] J. C. Roeske, L. Nuñez, M. Hoggarth, E. Labay, and R. R. Weichselbaum, "Characterization of the theorectical radiation dose enhancement from nanoparticles,"

Technology in cancer research & treatment, vol. 6, no. 5, p. 395–401, 2007. https://doi.org/10.1177/153303460700600504.

[11] T. Gray *et al.*, "A detailed experimental and Monte Carlo analysis of gold nanoparticle dose enhancement using 6 MV and 18 MV external beam energies in a macroscopic scale," *Applied Radiation and Isotopes*, vol. 171, p. 109638, 2021. https://doi.org/10.1016/j.apradiso.2021.109638.

[12] A. P. Klapproth, J. Schuemann, S. Stangl, T. Xie, W. B. Li, and G. Multhoff, "Multi-scale Monte Carlo simulations of gold nanoparticle-induced DNA damages for kilovoltage X-ray irradiation in a xenograft mouse model using TOPAS-nBio," *Cancer Nanotechnology*, vol. 12, no. 1, p. 27, 2021. https://doi.org/10.1186/s12645-021-00099-3.

[13] P. van Luijk, W. Dörr, and A. J. van der Kogel, "Tissue response models," in *Basic Clinical Radiobiology*: CRC Press, 2018, pp. 305–317. https://doi.org/10.1201/9780429490606.

[14] J. F. Fowler, "21 years of Biologically Effective Dose," *British Journal of Radiology*, vol. 83, no. 991, p. 554–568, 2010. https://doi.org/10.1259/bjr/31372149.

[15] O. F. Naismith *et al.*, "Forward- and Inverse-Planned Intensity-Modulated Radiotherapy in the CHHiP Trial: A Comparison of Dosimetry and Normal Tissue Toxicity," *Clinical Oncology*, vol. 31, no. 9, p. 600–610, 2019. https://doi.org/10.1016/j.clon.2019.05.002.

[16] F. Kazmi, K. A. Vallis, B. A. Vellayappan, A. Bandla, D. Yukun, and R. Carlisle, "Megavoltage Radiosensitization of Gold Nanoparticles on a Glioblastoma Cancer Cell Line Using a Clinical Platform," *International Journal of Molecular Sciences*, vol. 21, no. 2, p. 429 https://doi.org/10.3390/ijms21020429

[17] S. Devic, "Radiochromic film dosimetry: Past, present, and future," *Physica Medica: European Journal of Medical Physics*, vol. 27, no. 3, p. 122–134, 2011. https://doi.org/10.1016/j.ejmp.2010.10.001.

[18] P. Sipilä, J. Ojala, S. Kaijaluoto, I. Jokelainen, and A. Kosunen, "Gafchromic EBT3 film dosimetry in electron beams — energy dependence and improved film read-out," *Journal of Applied Clinical Medical Physics*, vol. 17, no. 1, p. 360–373, 2016. https://doi.org/10.1120/jacmp.v17i1.5970.

[19] L. Cui, S. Her, G. R. Borst, R. G. Bristow, D. A. Jaffray, and C. Allen, "Radiosensitization by gold nanoparticles: Will they ever make it to the clinic?," *Radiotherapy and Oncology*, vol. 124, no. 3, p. 344–356, 2017. https://doi.org/10.1016/j.radonc.2017.07.007.

[20] E. Vlastou, S. Diamantopoulos, and E. P. Efstathopoulos, "Monte Carlo studies in Gold Nanoparticles enhanced radiotherapy: The impact of modelled parameters in dose enhancement," *Physica Medica*, vol. 80, p. 57–64, 2020. https://doi.org/10.1016/j.ejmp.2020.09.022.

[21] H. Shen, H. Huang, and Z. Jiang, "Nanoparticle-based radiosensitization strategies for improving radiation therapy," (in English), *Frontiers in Pharmacology*, Review vol. Volume 14 - 2023, 2023. https://doi.org/10.3389/fphar.2023.1145551.